

MANEUVERABILITY AND HEADING CONTROL OF A QUADRUPED ROBOT UTILIZING TAIL DYNAMICS

Wael Saab

Robotics and Mechatronics Lab
Mechanical Engineering Dept.
Virginia Tech
Blacksburg, VA, USA

Pinhas Ben-Tzvi

Robotics and Mechatronics Lab
Mechanical Engineering Dept.
Virginia Tech
Blacksburg, VA, USA
bentzvi@vt.edu

ABSTRACT

This paper presents modeling and analysis of a quadruped robot that utilizes tail dynamics to control its heading angle. The tail is envisioned to assist locomotion as a means separate from its legs to generate forces and moments to improve performance in terms maneuverability. Tail motion is analyzed for both low and high-speed tail actuation to derive sufficient conditions to maintain equilibrium and formulate maneuverability relations that result in rotation and translation of the robotic system. Sensitivity analysis is presented to select optimal tail mass and length ratios to maximize the change of the heading angle. A heading controller is then proposed and simulated to achieve a desired heading angle utilizing tail dynamics. Results of this research will assist in the design, modeling, and analysis of robotic systems sharing similar topologies to the proposed model, such as mobile robots with wheeled, tracked, multi-legged, or articulated-body based locomotion with swinging extremities such as tails, torsos, and limbs.

1 INTRODUCTION

Biologists have long observed the uses and benefits that tails provide animals, which range from fat storage to communication [1]. Perhaps the most useful tail functionalities applicable to the field of mobile legged robotics are enhanced stabilization and maneuverability capabilities [2, 3]. Hickman [4] provided an extensive review of tail usage in mammals. For instance, kangaroos use their tails as a counterbalance while standing on their hind legs and as a means of energy storage to assist in hopping [5]. Kangaroo rats have been observed to rapidly swing their tails between hops to rotate their bodies in midair and continue hopping in a different direction. Dinosaurs, such as the Tyrannosaurus, are believed to have used their tails as an active counter balance and as a means of stabilization when walking forward, to maintain the yaw orientation of their

bodies [6, 7]. Similarly, cheetahs have been observed to swing their tails in rapid motions while chasing prey to maintain the roll of their bodies [8]. Lizards have also been observed to use their tails during aerial maneuvers to adjust their pitch for a smooth landing [9, 10].

By observing nature's abundant store of solutions, engineers can gain a source of inspiration in designing robots to address the challenges persisting in the field of legged robot design and control [11]. These challenges involve designing legged robots with high maneuverability and limited size, weight, and cost, and developing algorithms to control foot trajectories to achieve forward walking and turning gaits. The majority of research in the field of legged robotics has focused on the implementation of steady state trotting, galloping, and bounding [12-14]. We hypothesize that the burden on the legs to simultaneously stabilize and maneuver the robot can be reduced by utilizing an inertial appendage in the form of an attached tail. This can lead to simplifications of leg designs and control algorithms.

Various methods have been investigated to enhance maneuverability of mobile robots using an attached inertial appendage. A lizard-inspired tail has been successfully employed on a wheeled robot to dynamically self-right and control pitch to smoothly transition between various ground slopes, using the assumption of zero net angular momentum exchange [15, 16]. A similar approach was presented for a miniature jumping robot and a bio-inspired kangaroo robot with an active tail utilized for pitch control between jumping instances [17, 18]. A Newton-Euler approach was used to model a cheetah robot with a two degree-of-freedom (DOF) attached tail during mid-air flight. The authors developed and simulated an attitude controller and demonstrated preliminary experimental results of disturbance rejection to maintain stability [8]. A moth inspired robot successfully demonstrated self-righting and mid-air turning using an inertial appendage [19]. Patel et al. derived a

mathematical model of a wheeled robot with a single DOF tail capable of roll motion that was assumed to be rotating about a grounded pivot point using the Euler-Lagrange formulation. The authors developed a control algorithm and demonstrated with simulations that the robot could perform a high-speed roll faster than a tail-less robot [20]. The majority of research on robotic tails has focused on attitude control during mid-air flight using the zero-net transfer of angular momentum, an approach that has been extensively proposed in space robots and satellites for attitude control [21-23].

There has also been research conducted to analyze the dynamics of mobile robots with ground contact friction. Kohut et al. investigated dynamic turning of a hexapod robot using yaw motion of a tail [24, 25]. In this analysis, it was assumed that the tail torque occurs as soon as the tail is actuated that overwhelms static friction; therefore, dynamic friction between the feet and ground induces a moment about an effective radius during tail actuation. However, this model did not consider the effects of translation caused by inertial forces. Casarez et al. developed an analytical model of a mobile robot with a reaction wheel that transferred a pure moment, neglecting effects of inertial forces, to the robotic body to determine the effects of motor voltage, friction, and wheel inertia had on heading angle [26]. Chernous'Ko modeled multi-body mechanical systems consisting of several links which can perform snake-like locomotion's along a horizontal plane in the presence of dry friction. Periodic motions consisting of slow and fast phases were used to create controllable longitudinal, latitudinal translational and rotational motions using a sequence of elementary motions [27, 28].

This paper adapts the framework presented in [25, 27, 28] to model and analyze a robotic system consisting of a quadruped robot and swinging inertial appendage in the form of a tail. This paper is part of ongoing research that investigates the use of inertial tails on legged robots, which are envisioned to provide a means of external loading separate from the leg mechanisms, to generate forces and moments to aid maneuverability and stabilization [29-38]. The main contributions of this paper are: (1) modeling of the quadruped and swinging inertial appendage in the presence of friction to analyzes the effects of both low-speed and high-speed tail actuations on the robotic system in terms of maneuverability, defined as the resultant rotation and translation of the system, caused by both inertial forces and moments, (2) sensitivity analysis that utilizes the developed models to compute optimal tail mass and length ratios to maximize heading angle rotation of the legged robot, and (3) design and simulate a heading angle controller that utilizes tail dynamics.

This paper is organized as follows. Sections 2 and 3 present modeling and kinematic analysis of the robotic system. Section 4 presents dynamic analysis of low and high-speed tail actuations, to derive sufficient conditions to maintain equilibrium and the maneuverability relations to produce translation and rotation of the robotic system. Section 5 presents sensitivity analysis to compute optimal tail length and

mass ratios to maximize heading angle change. Section 6 presents simulation results of a heading angle controller. Concluding discussions are then presented in section 7.

2 ROBOTIC SYSTEM MODELING

This section presents the robotic system under study and the model that is used for analysis throughout this paper. Figure 1 shows a schematic diagram (side view) of robotic system that consists of a quadruped robot with an attached tail developed by the authors [37, 39]. The quadruped consists of four robotic modular legs that are designed to be low-inertia, two DOF mechanisms capable of performing planar walking gaits that enable planar forward locomotion. It is envisioned that rotation of the tail will enable to quadruped to adjust its heading angle for left and right turning as will be demonstrated in section 6. The quadruped's mass is concentrated in the body region due to the locations of its motors. It is assumed that during a walking gait the legs do not significantly change the mass properties of the robot. The tail is composed of an actuation unit that houses a geared motor assembly and a rigid rod with an attached tip mass.

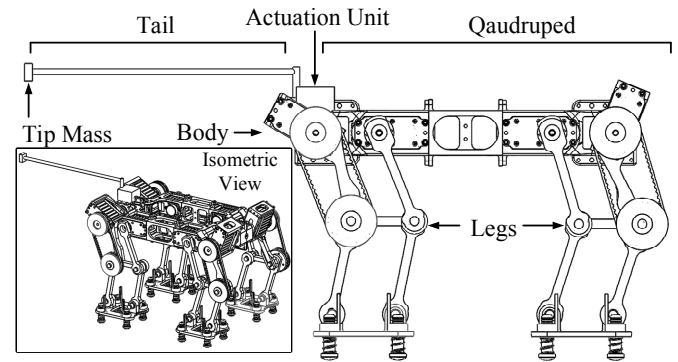


Figure 1. Schematic diagram of the robotic system composed of a quadruped and tail.

Figure 2 depicts the free body diagram (top view) of the robotic system. A body attached frame of reference ($O', \mathbf{b}_1, \mathbf{b}_2$) is fixed to the quadruped at $O' = (x_0, y_0)$. The bodies are modeled as point masses m_0 (actuation unit), m_1 (quadruped body), and m_2 (tail tip mass). In the figure, the quadruped and tail are disconnected at the tail revolute joint. The tail gearbox and actuator assembly is located at point O' . The bodies can translate in the inertial $\mathbf{e}_1\mathbf{e}_2$ -plane and the quadruped and tail can rotate relative to one another, about the \mathbf{e}_3 -axis. The heading angle of the quadruped and relative yaw angle of the tail are defined as θ and β , respectively. Therefore, the system is modeled with four DOFs.

The following variables will be used to represent the physical parameters of the system in this analysis: m_i represents lumped masses, \mathbf{v}_i is the mass velocities, and l_i represents effective radius, defined as half the diagonal distance between legs. The index $i = \{0, 1, 2\}$ refer to the actuation unit, quadruped, and tail bodies, respectively.

An input torque of magnitude M applied onto the tail produces yaw rotation about its revolute joint. A torque of equal magnitude and opposite direction acts on the quadruped body during tail actuation.

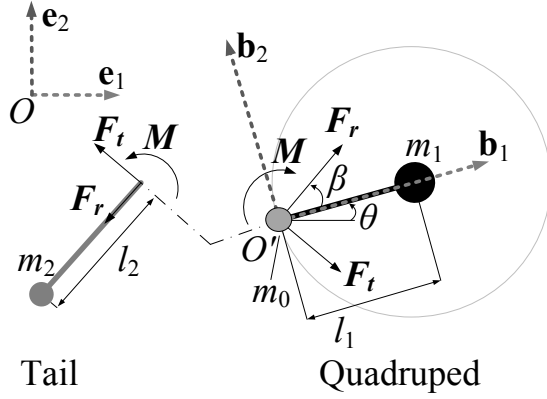


Figure 2. Free body diagram (top view) of the robotic system consisting of a quadruped robot and tail

Coulomb friction is used to model friction forces that act on the system at points of contact between the quadruped's feet and ground. During instances of sliding contact motion, the summation of friction forces is equal to μmg and opposes the direction of sliding velocity. Here, μ represents the friction coefficient (static and dynamic friction coefficients are assumed to be equivalent), m is the total mass of the system $m = m_0 + m_1 + m_2$, and g is the gravitational acceleration.

3 KINEMATIC ANALYSIS

This section presents kinematic analysis of the robotic system, and derivations of the center of mass location and angular momentum of the robotic system.

With reference to Fig. 2, the COM of the system is computed as follows

$$\begin{aligned} x_c &= \frac{mx_0 + m_1 l_1 \cos(\theta) - m_2 l_2 \cos(\theta + \beta)}{m} \mathbf{e}_1 \\ y_c &= \frac{my_0 + m_1 l_1 \sin(\theta) - m_2 l_2 \sin(\theta + \beta)}{m} \mathbf{e}_2 \end{aligned} \quad (1)$$

By defining the angular velocities of the quadruped and tail to be $\boldsymbol{\omega}_1 = \dot{\theta} \mathbf{e}_3$ and $\boldsymbol{\omega}_2 = \dot{\theta} + \dot{\beta} \mathbf{e}_3$, the total angular momentum of the robotic system about point O is given by Eq. (2)

$$\mathbf{H}_O = \sum_{i=0}^3 m_i \mathbf{R}_i \times \mathbf{v}_i \quad (2)$$

Substituting position and velocity relations into the above equation and evaluating the cross products yields the total angular momentum of the system:

$$\begin{aligned} \mathbf{H}_O &= (\sin(\theta) l_1 m_1 (y_0 \dot{\theta} - \dot{x}_0) + \cos(\theta) l_1 m_1 (x_0 \dot{\theta} + \dot{y}_0) \\ &\quad - l_2 m_2 [\cos(\beta + \theta) x_0 (\dot{\beta} + \dot{\theta}) + \sin(\beta + \theta) (y_0 (\dot{\beta} + \dot{\theta}) - \dot{x}_0) \\ &\quad + \cos(\beta + \theta) \dot{y}_0] - m y_0 \dot{x}_0 - m x_0 \dot{y}_0) \mathbf{e}_3 \end{aligned} \quad (3)$$

4 DYNAMIC ANALYSIS

This section analyses low and high-speed tail actuation to determine the conditions required to maintain equilibrium and derive the relations of maneuverability that result in translation and rotation of the robotic system.

Analysis of this low-speed tail motion will study the forces and moments produced by the tail to determine the conditions required to maintain equilibrium. Low-speed tail actuation involves rotating the tail to desired initial conditions while maintaining equilibrium. Equilibrium refers to steady state conditions where the system remains stationary due to resistive friction forces. To maneuver, a high-speed tail actuation will be performed to generate the necessary forces and moments to overcome friction. Let the magnitude of the moment induced by friction forces be denoted by M_f . During this type of actuation, it is assumed that the input torque magnitude is larger than the friction induced moment $M > M_f$; therefore, the external frictional forces between the quadruped's feet and ground can be neglected; thus, satisfying the conservation laws of linear and angular momentum. Since the system is initially at equilibrium, after fast tail motions, \mathbf{x}_c and \mathbf{y}_c are constants of motion and $\mathbf{H}_O = \mathbf{0}$. These conservation laws will then be used to analyze high-speed tail actuation, to formulate relations of maneuverability in terms of variations of translation and rotation of the robotic system.

4.1 Low-Speed Tail Actuation

In this section we formulate the conditions to maintain equilibrium during low-speed tail actuation. Assuming that the system is initially at equilibrium, we first estimate the upper bound of generated forces from tail actuation and use them to analyze the resultant force balance on the quadruped, to determine the maximum threshold of tail motion such that friction induced forces cancel those caused by the actuator torque and loading generated by the tail.

For low-speed tail actuation, the maximum generated forces resulting from tail actuation that maintain system equilibrium occur at a certain upper, maximum threshold of tail motion parameters defined by ε and Ω , which represent the magnitude of angular velocity and acceleration, respectively. Using this notation and considering the tail as the system of study, the maximum magnitudes of F_t and F_r , tangential and radial force magnitude components exerted on the tail by the quadruped, and M can be estimated by

$$\begin{aligned} F_r &\leq m_2 l_2 \varepsilon^2 \\ F_t &\leq m_2 l_2 \Omega \\ M &\leq m_2 l_2^2 \Omega \end{aligned} \quad (4)$$

We now study the effects of these maximum forces and moment on the quadruped consisting of masses m_0 and m_1 . Rotational equilibrium will be maintained if the magnitude of the maximum induced moment \mathbf{M}_1 , composed of the input torque and the moment resulting from maximum generated forces \mathbf{F}_t and \mathbf{F}_r , about the combined COM does not exceed the friction induced moment magnitude M_f . Translational equilibrium will be maintained if the magnitude of the maximum combined generated forces, \mathbf{F}_1 , does not exceed the friction force magnitude F_f . This means that the generated loading due to the low speed-tail actuation will not cause the quadruped to maneuver, since it is opposed by the friction induced forces and moments. Therefore, the conditions to maintain equilibrium are defined as

$$\begin{aligned} |\mathbf{F}_1| &\leq F_f \\ |\mathbf{M}_1| &\leq M_f \end{aligned} \quad (5)$$

A balance of forces and moments about the combined COM with respect to the body attached frame yields the following equation for \mathbf{F}_1 and \mathbf{M}_1

$$\begin{aligned} \mathbf{F}_1 &= (F_r \cos \beta + F_t \sin \beta) \mathbf{b}_1 + (F_r \sin \beta - F_t \cos \beta) \mathbf{b}_2 \\ \mathbf{M}_1 &= [x_c (F_t \cos \beta - F_r \sin \beta) - M + y_c (F_t \sin \beta + F_r \cos \beta)] \mathbf{b}_3 \end{aligned} \quad (6)$$

Substituting Eq. 4 into Eq. 6 and using the Cauchy-Schwarz inequality, relations for $|\mathbf{F}_1|$ and $|\mathbf{M}_1|$ can be defined as

$$\begin{aligned} |\mathbf{M}_1| &\leq m_2 l_2^2 \Omega + 2m_2 l_2 \left(\frac{m_1 l_1 + m_2 l_2}{m} \right) (\Omega + \varepsilon^2) \\ |\mathbf{F}_1| &\leq m_2 l_2 \sqrt{\Omega^2 + \varepsilon^4} \end{aligned} \quad (7)$$

For multi legged robotic systems, F_f can be estimated as a force proportional to the total weight of the robotic system mg and μ . Similarly, M_f is proportional to F_f and the effective radius l_1 . Substituting these relations and Eq. 7 back into Eq. 5 yields the necessary condition to maintain equilibrium:

$$\begin{aligned} m_2 l_2^2 \Omega + 2m_2 l_2 \left(\frac{m_1 l_1 + m_2 l_2}{m} \right) (\Omega + \varepsilon^2) &\leq \mu mg l_1 \\ m_2 l_2 \sqrt{\Omega^2 + \varepsilon^4} &\leq \mu mg \end{aligned} \quad (8)$$

If the above inequalities are satisfied, the system will maintain equilibrium and remain stationary, enabling the robotic system to position the tail during low-speed tail actuation prior to maneuvering using high-speed tail actuation.

4.2 High-Speed Tail Actuation

In this section, the laws of conservation of linear and angular momentum, discussed in Section 4, are applied to derive the relations of maneuverability during high-speed tail actuation. Using the relation $\dot{x}_c = \dot{y}_c = \mathbf{0}$ from conservation laws, the time derivative of Eq. 1 is computed to derive the velocity of point mass m_0 :

$$\begin{aligned} \dot{\mathbf{x}}_0 &= \frac{m_1 l_1 \dot{\theta} \sin \theta - m_2 l_2 (\dot{\theta} + \dot{\beta}) \sin(\theta + \beta)}{m} \mathbf{e}_1 \\ \dot{\mathbf{y}}_0 &= \frac{-m_1 l_1 \dot{\theta} \cos \theta + m_2 l_2 (\dot{\theta} + \dot{\beta}) \cos(\theta + \beta)}{m} \mathbf{e}_2 \end{aligned} \quad (9)$$

Substituting Eq. 9 into the relation for total angular momentum, Eq. 3, where $\mathbf{H}_0 = \mathbf{0}$ due to conservation laws, yields an expression for the heading angle rate of change

$$\dot{\theta} = - \frac{l_2^2 m_2 (m_0 + m_1) + d}{m_1 l_1^2 (m_0 + m_2) + m_2 l_2^2 (m_0 + m_1) + 2d} \dot{\beta} \quad (10)$$

Where $d = l_1 l_2 m_1 m_2 \cos \beta$. It can be observed from Eq. 10 that $\Delta \theta$ is inversely related to $\Delta \beta$. This relation is intuitive since any action of the tail will have an equal and opposite reaction on the quadruped. Numerical integration of Eq. 10 yield the relation of heading angle variation defined by

$$\Delta \theta = - \int_{\beta_i}^{\beta_f} f(\beta) d\beta \quad (11)$$

where β_i and β_f represent the initial and final values of β . By integrating Eq. 9 over the initial and final values of tail motion, the translation of the system is computed to be

$$\begin{aligned} \Delta \mathbf{x}_0 &= \frac{-m_1 a_1 \Delta \cos \theta + m_2 a_2 \Delta \cos(\theta + \beta)}{m} \mathbf{e}_1 \\ \Delta \mathbf{y}_0 &= \frac{-m_1 a_1 \Delta \sin \theta + m_2 a_2 \Delta \sin(\theta + \beta)}{m} \mathbf{e}_2 \end{aligned} \quad (12)$$

Equations (11) and (12) represent maneuverability relations of the legged robot due to high-speed tail actuations.

5 HEADING ANGLE SENSITIVITY ANALYSIS

The maneuverability relations derived in this section are applicable to a wide range of mobile robots that utilize dynamics of a tail. This section analyses the sensitivity of the tail mass and length ratios, defined as $\sigma = m_2 / (m_0 + m_1)$, $\lambda = l_2 / l_1$, on the variation of heading angle.

For a quadruped of mass $m_1 = 13$ kg, $m_0 = 2$ kg and effective radius $l_1 = 0.5$ m, Eq. (11) was evaluated for $\Delta \beta = \pi / 2$ rad. Figure 3 shows the plot of heading angle vs. mass ratio for various length ratio values $\lambda = \{0.5, 1, 2, 3, 4\}$.

From the plot, it can be observed that increasing the values of β and λ does increase $\Delta\theta$, since the variation of heading angle changes with design parameters and reaches near steady state conditions. For example, past a certain mass ratio threshold of $\sigma \sim 0.025$, the addition of tail mass does not significantly cause large variations of heading angle, since the slope of $\Delta\theta$ nearly approaches zero. This trend physically makes sense because tail mass does increase the inertial forces transferred to the quadruped, but also increases the overall weight of the system, resulting in a larger friction induced moment that impedes motion of the system. It can be observed that heading angle is more sensitive to the tail length ratio. This sensitivity can be seen in Fig. 3 by observing the large differences between steady state $\Delta\theta$ values as λ increases. However as λ is increased beyond a threshold $\lambda \sim 2$, the effectiveness of heading angle variation decreases. This trend can be physically explained due to the quadratic increase of tail inertia with respect to tail length; however, inertial forces in the tangential and radial directions also affect $\Delta\theta$, as seen in Fig. 2, and are expected to limit the variation of heading angle for large values of λ .

Therefore, the most effective means to obtain large variations of heading angle is to maximize tail length while satisfying dimension constraints. Results of this analysis can be used to effectively size a robotic tail for a given legged robot of known mass and dimensions.

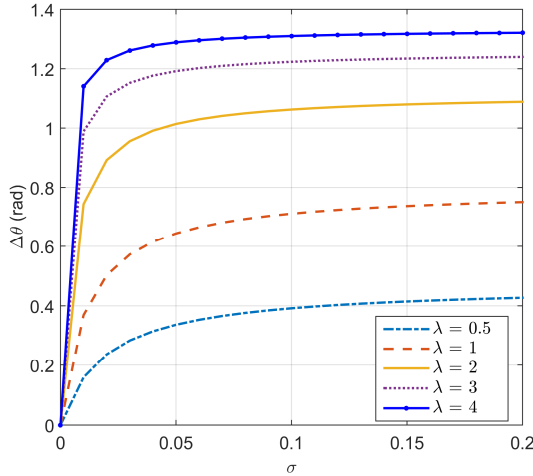


Figure 3. Plot of heading angle vs. mass ratio for various length ratio values.

6 HEADING CONTROLLER

The robotic system is modeled as four DOFs with one active DOF in the form of torque input to the tail. Therefore, the system is under actuated. At this stage, the heading angle of the quadruped will be deemed the most important and a controller will be designed to close the loop on this variable; hence, the remaining DOF's will be uncontrolled.

As a preliminary approach to designing a heading angle controller, we choose to implement a linear quadratic regulator (LQR). For ease of simulation, the time derivative of Eq. 10 was computed and linearized using a small angle

approximation $\ddot{\beta} = u/m_2 l_2^2$ and put into state space form with the state vector defined as $[\theta, \dot{\theta}]$. The gains of the LQR controller were manually tuned to produce acceptable rise time and settling time for a desired heading angle θ_{des} , and input saturation u_{sat} was incorporated to better approximate actuator performance.

Simulation parameters of the physical system, Fig. 1, were obtained from CAD software as: $m_0 = 2$ kg, $m_1 = 13$ kg, $m_2 = 0.3$ kg, $l_1 = 0.5$ m, $l_2 = 1$ m. Quadruped mass parameters were extracted from computer aided design software. The tail mass and length ratios were chosen based off the analysis in section 5 such that $\sigma = 0.02$ and $\lambda = 2$. Figure 4 shows simulation results of heading angle and heading angular velocity for desired heading angle set point values $\theta_d = \{\pi/8, \pi/4, \pi/2\}$ rad and $u_{sat} = \pm 15$ Nm. Figure 5 shows the simulation results of the resultant tail angle for the three desired heading angle set points. From Figs. 4 and 5 it can be observed that: 1) the LQR controller rise time is approximately equivalent to 3 s for all three case scenarios although θ_d is increasing, this results in a higher tail angular velocity $\dot{\beta}$ to achieve the desired set-points, 2) β increases inversely proportional with respect to θ_d as expected from Eq. 10. These results can be used to design the physical system for experimentation. For example, the high requirements of $\dot{\beta}$ magnitudes must be practically achieved by the chosen geared motor based on specifications and the tail must be designed to avoid interference with the quadruped body for large desired heading angle values based on simulated results of the resultant β angular displacements or the control algorithm should be modified to account for a limited tail range of motion.

Using the resultant tail angular profiles in Fig. 5, the expected translation of the system can be computed using Eq. 12. Computed results of translation of the robotic system are presented in Table 1.

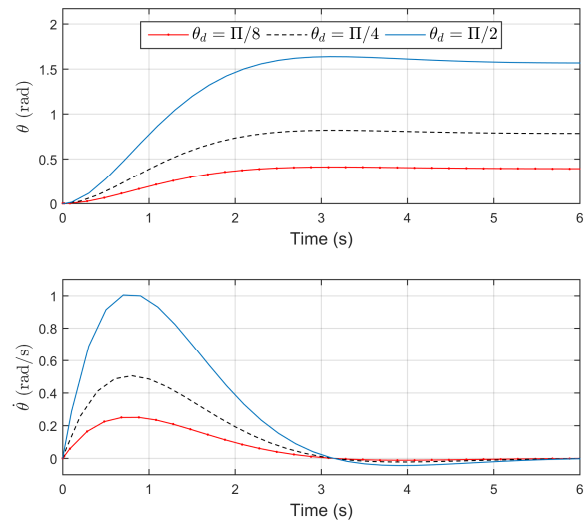


Figure 4. Simulation results of heading angle and velocity for various θ_d set point values.

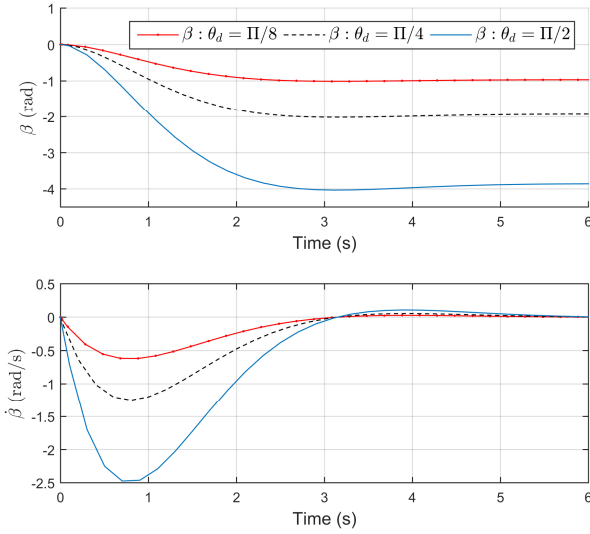


Figure 5. Simulation results of tail angle and velocity for various θ_d set point values.

Table 1. Computed translation of the robotic system due to tail rotation.

θ_d (rad)	$\{\beta_i, \beta_f\}$ (rad)	Δx_0 (cm)	Δy_0 (cm)
$\pi/8$	$\{0, -0.96\}$	2.0	-15.3
$\pi/4$	$\{0, -1.9\}$	0.4	-16.1
$\pi/2$	$\{0, -3.8\}$	-1.3	-13.5

7 CONCLUSION

In this paper, we analyzed a robotic system composed of a quadruped robot and an attached tail that is used to provide a means separate from its legs to generate external forces and moments to maneuver and control the heading angle. Modeling and analysis of the system was performed, where sufficient conditions to maintain equilibrium and produce maneuverability using low and high-speed tail actuations were derived. Using the derived expression of heading angle variation, sensitivity analysis of heading angle dependent on design parameters was presented and an LQR controller was implemented to control heading angle.

Results of this analysis can be used to choose tail length and mass ratios to maximize the variation of heading angle utilizing tail dynamics. Simulation results of the tail angular displacement and velocities will be used in designing a physical prototype of the robotic system and will aid the process of actuators selection. Future work will involve expanding the kinematic and dynamic models to analyze the effects of articulated tail structures as opposed to the single bodied rigid pendulum model used in this paper. A nonlinear controller will be developed to more accurately estimate the response of the system.

ACKNOWLEDGMENTS

This material is based upon work supported by the National Science Foundation under Grant No. 1557312.

REFERENCES

- [1] Aleksiuik, M., 1968, "Scent-Mound Communication, Territoriality, and Population Regulation in Beaver " *Journal of Mammalogy*, 49(4), pp. 759-762.
- [2] Jindrich, D. L., and Qiao, M., 2009, "Maneuvers During Legged Locomotion," *Chaos: An Interdisciplinary Journal of Nonlinear Science*, 19(2), p. 026105.
- [3] Webb, P. W., 2004, "Maneuverability-General Issues," *IEEE Journal of Oceanic Engineering*, 29(3), pp. 547-555.
- [4] Hickman, G. C., 1979, "The Mammalian Tail: A Review of Functions," *Mammal review*, 9(4), pp. 143-157.
- [5] Proske, U., 1980, "Energy Conservation by Elastic Storage in Kangaroos," *Endeavour*, 4(4), pp. 148-153.
- [6] Howell, A. B., 1944, "Speed in Animals, Their Specialization for Running and Leaping," *American Journal of Physical Anthropology*, 3(1).
- [7] Benton, M. J., 2010, "Studying Function and Behavior in the Fossil Record," *PLoS biology*, 8(3).
- [8] Briggs, R., Lee, J., Haberland, M., and Kim, S., 2012, "Tails in Biomimetic Design: Analysis, Simulation, and Experiment," *Proc. International Conference on Intelligent Robots and Systems IEEE/RSJ, Vilamoura, Algarve Portugal*, pp. 1473-1480.
- [9] Jusufi, A., Kawano, D., Libby, T., and Full, R., 2010, "Righting and Turning in Mid-Air Using Appendage Inertia: Reptile Tails, Analytical Models and Bio-Inspired Robots," *Bioinspiration and Biomimetics*, 5(4), p. 045001.
- [10] Libby, T., Moore, T. Y., Chang-Siu, E., Li, D., Cohen, D. J., Jusufi, A., and Full, R. J., 2012, "Tail-Assisted Pitch Control in Lizards, Robots and Dinosaurs," *Nature*, 481(7380), pp. 181-184.
- [11] Bowling, A., 2011, "Impact Forces and Agility in Legged Robot Locomotion," *Journal of Vibration and Control*, 17(3), pp. 335-346.
- [12] Kazemi, H., Majd, V. J., and Moghaddam, M. M., 2013, "Modeling and Robust Backstepping Control of an Underactuated Quadruped Robot in Bounding Motion," *Robotica*, 31(03), pp. 423-439.
- [13] Krasny, D. P., and Orin, D. E., 2013, "Evolution of Dynamic Maneuvers in a 3d Galloping Quadruped Robot," *Proc. International Conference on Robotics and Automation, IEEE, Orlando, FL, USA*, pp. 1084-1089.
- [14] Wang, X., Li, M., Wang, P., and Sun, L., 2011, "Running and Turning Control of a Quadruped Robot with Compliant Legs in Bounding Gait," *Proc. IEEE International Conference on Robotics and Automation IEEE, Shanghai, China*, pp. 511-518.
- [15] Chang-Siu, E., Libby, T., Tomizuka, M., and Full, R. J., 2011, "A Lizard-Inspired Active Tail Enables Rapid Maneuvers and Dynamic Stabilization in a Terrestrial Robot," *Proc. International Conference on Intelligent*

- Robots and Systems*, IEEE/RSJ, San Francisco, CA, USA, pp. 1887-1894.
- [16] Johnson, A. M., Libby, T., Chang-Siu, E., Tomizuka, M., Full, R. J., and Koditschek, D. E., 2012, "Tail Assisted Dynamic Self Righting," *Proc. International Conference on Climbing and Walking Robots and the Support Technologies for Mobile Machines*, Springer, Baltimore, MD, USA.
- [17] Liu, G.-H., Lin, H.-Y., Lin, H.-Y., Chen, S.-T., and Lin, P.-C., 2014, "A Bio-Inspired Hopping Kangaroo Robot with an Active Tail," *Journal of Bionic Engineering*, 11(4), pp. 541-555.
- [18] Zhao, J., Zhao, T., Xi, N., Cintrón, F. J., Mutka, M. W., and Xiao, L., 2013, "Controlling Aerial Maneuvering of a Miniature Jumping Robot Using Its Tail," *Proc. International Conference on Intelligent Robots and Systems IEEE/RSJ*, Tokyo, Japan, pp. 3802-3807.
- [19] Demir, A., ANKARALI, M. M., Dyhr, J., Morgansen, K., Daniel, T., and Cowan, N., 2012, "Inertial Redirection of Thrust Forces for Flight Stabilization," *Proc. International Conference on Climbing and Walking Robots and Support Technologies for Mobile Machines*, Springer, Baltimore, MD, USA, pp. 239-245.
- [20] Patel, A., and Braae, M., 2013, "Rapid Turning at High-Speed: Inspirations from the Cheetah's Tail," *Proc. International Conference on Intelligent Robots and Systems* Tokyo, Japan, pp. 5506-5511.
- [21] Fernandes, C., Gurvits, L., and Li, Z., 1993, "Attitude Control of Space Platform/Manipulator System Using Internal Motion," *Space Robotics: Dynamics and Control*, Springer, pp. 131-163.
- [22] Papadopoulos, E., and Dubowsky, S., 1991, "On the Nature of Control Algorithms for Free-Floating Space Manipulators," *IEEE Transactions on Robotics and Automation*, 7(6), pp. 750-758.
- [23] Yoshida, K., and Umetani, Y., 1990, "Control of Space Free-Flying Robot," *Proc. Conference on Decision and Control*, IEEE, Honolulu, HI, USA, pp. 97-102.
- [24] Kohut, N., Haldane, D., Zarrouk, D., and Fearing, R., 2012, "Effect of Inertial Tail on Yaw Rate of 45 Gram Legged Robot," *Proc. International Conference on Climbing and Walking Robots and the Support Technologies for Mobile Machines*, Springer, Baltimore, MD, USA, pp. 157-164.
- [25] Kohut, N. J., Pullin, A. O., Haldane, D. W., Zarrouk, D., and Fearing, R. S., 2013, "Precise Dynamic Turning of a 10 Cm Legged Robot on a Low Friction Surface Using a Tail," *Proc. IEEE International Conference on Robotics and Automation*, IEEE, Karlsruhe, Germany, pp. 3299-3306.
- [26] Casarez, C., Penskiy, I., and Bergbreiter, S., 2013, "Using an Inertial Tail for Rapid Turns on a Miniature Legged Robot," *Proc. International Conference on Robotics and Automation IEEE*, Karlsruhe, Germany, pp. 5469-5474.
- [27] Chernous'ko, F., 2005, "Modelling of Snake-Like Locomotions," *Modeling, Simulation and Optimization of Complex Processes*, pp. 105-114.
- [28] Chernous'ko, F., 2001, "Controllable Motions of a Two-Link Mechanism Along a Horizontal Plane," *Journal of Applied Mathematics and Mechanics*, 65(4), pp. 565-577.
- [29] Rone, W. S., and Ben-Tzvi, P., 2012, "Continuum Manipulator Statics Based on the Principle of Virtual Work," *Proc. International Mechanical Engineering Congress and Exposition*, ASME, Houston, TX, USA, pp. 321-328.
- [30] Rone, W. S., and Ben-Tzvi, P., 2013, "Multi-Segment Continuum Robot Shape Estimation Using Passive Cable Displacement," *Proc. International Symposium on Robotic and Sensors Environments*, IEEE, Washington, DC, USA, pp. 37-42.
- [31] Rone, W. S., and Ben-Tzvi, P., 2014, "Continuum Robotic Tail Loading Analysis for Mobile Robot Stabilization and Maneuvering," *Proc. International Design Engineering Technical Conferences & Computers and Information in Engineering Conference*, ASME, Buffalo, NY, USA, pp. V05AT08A009-V005AT008A009.
- [32] Rone, W. S., and Ben-Tzvi, P., 2014, "Mechanics Modeling of Multisegment Rod-Driven Continuum Robots," *ASME Journal of Mechanisms and Robotics*, 6(4), p. 041006.
- [33] Rone, W. S., and Ben-Tzvi, P., 2014, "Continuum Robot Dynamics Utilizing the Principle of Virtual Power," *IEEE Transactions on Robotics*, 30(1), pp. 275-287.
- [34] Rone, W. S., and Ben-Tzvi, P., 2015, "Static Modeling of a Multi-Segment Serpentine Robotic Tail," *Proc. International Design Engineering Technical Conferences and Computers and Information in Engineering Conference*, ASME, Boston, MA, USA, pp. V05AT08A054-V005AT008A054.
- [35] Rone, W. S., and Ben-Tzvi, P., 2016, "Dynamic Mobile Robot Maneuvering Utilizing Tail-Induced Inertial Loading," *ASME Journal of Dynamic Systems Measurement and Control*
- [36] Saab, W., and Ben-Tzvi, P., 2016, "Design and Analysis of a Discrete Modular Serpentine Tail," *Proc. International Design Engineering Technical Conferences & Computers and Information in Engineering Conference*, ASME, Charlotte, NC, USA, p. 8.
- [37] Saab, W., and Ben-Tzvi, P., 2016, "Design and Analysis of a Robotic Modular Leg," *Proc. International Design Engineering Technical Conferences & Computers and Information in Engineering Conference*, ASME, Charlotte, NC, USA, p. 8.
- [38] Saab, W., Rone, W., and Ben-Tzvi, P., 2017, "Discrete Modular Serpentine Robotic Tail: Design, Analysis and Experimentation," *Robotica*.
- [39] Saab, W., Rone, W., and Ben-Tzvi, P., 2016, "Robotic Modular Leg: Design, Analysis and Experimentation," *Journal of Mechanisms and Robotics*.